

<https://doi.org/10.22226/2410-3535-2023-1-45-49>

Modelling of disclinated phosphorene crystals

M. A. Rozhkov^{†,1}, N. D. Abramenko¹, A. M. Smirnov¹, A. L. Kolesnikova^{1,2}, A. E. Romanov¹

[†]MA.Rozhkov@itmo.ru

¹ITMO University, St. Petersburg, 197101, Russia

²Institute for Problems in Mechanical Engineering RAS, St. Petersburg, 199178, Russia

In this article, the disclinated modifications of two-dimensional phosphorene crystals are modelled. The modelling technique explores the crystal lattices of disclinated graphenes known as pseudo-graphenes to form a family of materials sharing the same lattice structure and symmetry. To design crystal lattice of disclinated phosphorenes Ph5-7v1 and Ph5-6-7v2, the structures of pseudo-graphenes G5-7v1 and G5-6-7v2 are chosen as reference ones, respectively. Optimization procedure done with density functional theory (DFT) calculations proves that the designed lattices of disclinated phosphorenes are structurally stable that allows to analyze the band structure of phosphorene allotropes under consideration.

Keywords: phosphorene, disclination, disclinated phosphorene, band structure.

1. Introduction

The discovery of graphene and two decades of graphene studies stimulated a great interest to other two-dimensional (2D) materials such as phosphorene, molybdenum disulfide, germanene, stanene and silicene [1,2]. Prediction of properties and modelling of 2D materials is a relatively novel and promising field in condensed matter physics and materials science due to exotic functional characteristics of such materials and their prospects for electronics and optoelectronics [3–5]. For instance, graphene possesses unusual electronic properties [6], has a high thermal conductivity [7] and demonstrates a unique set of mechanical characteristics [8].

During the last decade, studies on graphene with defects — point defects, dislocations, disclinations, and grain boundaries as well as on various graphene allotropes — periodic pseudo-graphene structures were emerged [9–11]. Defects generated in the processes of fabrication and exploitation of graphene structures change their functional properties. For example, the conductivity associated with the graphene grain boundary is an order of magnitude lower than for the defect-free graphene [12]. In the same way, biphenylene — pseudo-graphene material, i.e., a 2D crystal consisting not only of 6-member carbon rings, but also of 4-, 6-, and 8-member disclinated (defective) carbon rings, obtained experimentally [13] and described theoretically [14] in 2021, has properties significantly different from those of graphene. Pseudo-graphene structures were theoretically studied since 1998 [15] including phagraphene [16] — the most known example of them. A detailed classification of pseudo-graphenes has been recently proposed in [11]. The classification utilized the disclination network approach. While there exist a plenty of studies regarding the influence of defects on the characteristics of graphene and pseudo-graphenes, the issue remains relevant for other 2D materials.

Our global research efforts pursue the modeling of new non-carbon 2D materials with periodic arrangements of

disclination defects. In this article, we perform a theoretical study of several new allotropic modifications of phosphorene, namely, disclinated phosphorenes. Previously, only isolated defects were theoretically considered in phosphorene [17,18]. Some polymorphs of phosphorene were also discussed in [19].

As it was shown in our studies (see [10,11]), the disclination approach has proven to be a valuable tool in pseudo-graphene modelling. For disclinated phosphorenes, we would like to see how the periodic arrangements of disclinations affect the properties of these new materials, such as the electronic band structure, in comparison to the role of the same defects played for pseudo-graphenes. For the current analysis, the lattices of G5-7v1 and G5-6-7v2 pseudo-graphene crystals (in accordance with the nomenclature advanced in [11]) were used to model new 2D materials originated from phosphorene.

2. Background. Pseudo-graphenes — graphene with disclinations

It is known that defects in graphene are associated with carbon atom rings with a local axial symmetry that is different from the hexagonal one. For example, the Stone-Wales defect, which is formed by a 90° rotation change in the relative positions of two atoms in the graphene lattice, is a combination of two 5-member and two 7-member carbon atom rings [20]. The defective carbon atom rings can be described by introducing/removing a wedge with angle that is a multiple of $\pi/3$ in graphene lattice built on hexagonal carbon atom ring. In physics and mechanics of solids the procedure with material wedge manipulations leads to the formation of specific defects known as wedge disclinations [21, 22]. The 5- and 7-member carbon atom rings correspond to wedge disclinations with the strengths $\omega = +\pi/3$ and $\omega = -\pi/3$, respectively, see Fig. 1. The 4- and 8-member carbon atom rings are described by disclinations with the strengths $\omega = \pm 2\pi/3$, where positive sign corresponds to the

4-member carbon atom ring, and negative to the 8-member one. Using of disclinated carbon atom rings and accounting for the properties of disclinations provide a convenient and illustrative approach for describing the structure and characteristics of graphene with defects [10, 23, 24].

Isolated disclinations in elastic bodies produce distortions of the material that diverge not only at the defect core but also at large distances from the defect [21]. According to their properties [25], disclinations tend to form screened arrangements in crystalline bodies, where the elastic fields of opposite signed defects will overlap [21–23]. In [10], possible configurations of disclinations in graphene were considered, which can act as structural units (Fig. 2 a) for the construction of higher order defects, such as grain boundaries, see Fig. 2 b, or intergrain interfaces. These high order defects can also form two-dimensional arrays, creating carbon atom crystals with a high density of disclinations, i.e. pseudo-graphenes, see Fig. 2 c.

The pseudo-graphene crystal lattice is designed by embedding periodic arrays of positive and negative wedge disclinations, respectively, into the graphene lattice [23].

In general, pseudo-graphene is a two-dimensional carbon crystal consisting mainly of non-hexagonal carbon atom rings, which are arranged according to a periodic law. According to pseudo-graphene classification, proposed in [11], these periodic carbon atom structures could be described by their form-factor, hybridization and electronic structure type. For instance, G5-7v1 pseudo-graphene consists of 5 and 7-member rings of sp^2 -hybridized carbon atoms and demonstrates semimetal electronic band structure [26], on the other hand, G4-8v1 pseudo-graphene contains 4 and 8-member rings of sp^2 -hybridized carbon atoms and possesses the band structure being typical for metals [27]. It should be noted that the changes in the band structure indicates the possibility of controlling the characteristics of graphene-like 2D materials.

3. Modelling techniques

To analyze atomic configurations and the band structures of the disclinated phosphorene, the DFT based Quantum Espresso software package [28] with generalized gradient

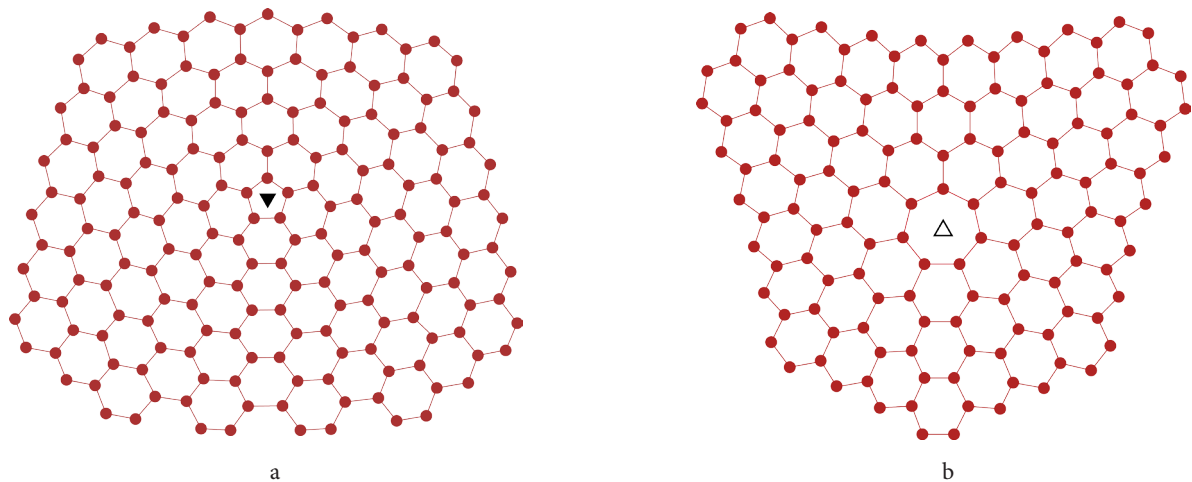


Fig. 1. Disclinations in graphene. Positive disclination (filled triangle) of strength $\omega = +\pi/3$ (a); negative disclination (empty triangle) of strength $\omega = -\pi/3$ (b).

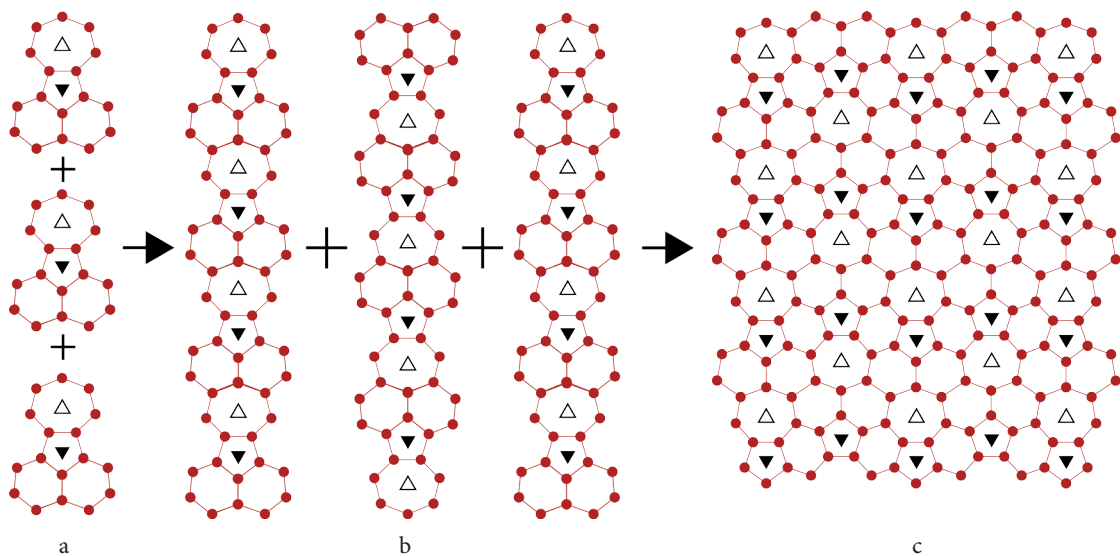


Fig. 2. Assembly of a pseudo-graphene crystal G5-6-7v2 from structural units: a chain of structural units is combined into a grain boundary (a); grain boundaries are used as structural elements to create a pseudo-graphene crystal (b); pseudo-graphene crystal G5-6-7v2 (c). Disclinations in structural units, grain boundaries, and pseudo-graphenes are shown as triangles.

approximation (GGA) was exploited using the Perdew-Burke-Ernzerhof (PBE) exchange-correlation functional. The plane-wave cut-off energy was set to 500 eV. Brillouin zone integration is performed with Monkhorst-pack Gamma-centered k-space mesh of size $7 \times 7 \times 1$. We used k-space mesh gap of value 0.005 \AA^{-1} for electronic band structure calculation. The simulation cell contained a single sheet and a vacuum barrier of 20 \AA in Z-direction, so that there was no physical interaction between periodic parts of the model along Z-coordinate.

The initial lattice structures for the disclinated phosphorene crystals were built basing on the structural units of G5-7v1 and G5-6-7v2 for pseudo-graphene crystals [11]. In order to prepare the structure for disclinated phosphorene, we followed the algorithm described in [29]. We first got the coordinate representation of the chosen pseudo-graphene crystal structure that was either G5-6-7v2, or G5-7v1. To explore the method, one only needs the data for the pseudo-graphene unit cell. After the coordinates were gathered, we performed the following atomic manipulations. First, we shifted half of the phosphorus atoms along the Z-coordinate to reproduce the “two-level” nature of phosphorene. We then scaled the phosphorus atom coordinates using the ratio of phosphorene to graphene lattice parameters $r = 3.27 \text{ \AA} / 2.46 \text{ \AA} = 1.33$, where 2.46 \AA is a lattice parameter for graphene [30, 31] and 3.27 \AA is a lattice parameter for phosphorene [19]. As the final step, the resulting unit cell of the phosphorus atom-based material was replicated several times in X and Y dimensions to form a new simulation box, which was used in our DFT calculations.

4. Geometry of disclinated phosphorenes

To realize the outlined approach, we considered structural units and elementary lattice cells of pseudo-graphenes G5-7v1 and G5-6-7v2, see Fig. 3. The G5-6-7v2 pseudo-graphene crystal has lattice parameters equal to $a = 8.22 \text{ \AA}$ and $b = 6.48 \text{ \AA}$; for such a pseudo-graphene disclinations lead predominantly to distortions of defect-free hexagonal (6-member) carbon atom rings. The G5-7v1 pseudo-graphene crystal has lattice parameters equal to $a = 7.38 \text{ \AA}$ and $b = 5.81 \text{ \AA}$; in this case defect-free graphene-like carbon atom rings are completely absent. These two atomic configurations serve as a basis for the lattice design of new 2D materials.

To build the atomic structure of disclinated phosphorenes, we started with a “raw” description of crystal lattices (appearance and atomic coordinates) using the procedure described in Section 3, in which each carbon atom in the pseudo-graphene was replaced by a pair of phosphorus atoms. For this ‘raw’ data, we then performed crystal lattice geometry optimization. We designate these new 2D materials following our classification proposed in [11] for pseudo-graphenes: Ph5-6-7v2 and Ph5-7v1, respectively. It is worth to note that the atomic structure of Ph5-6-7v2 material was discussed in detail in [29].

In Fig. 4a we give the crystal lattice for pristine phosphorene; it possesses lattice parameters $a = 3.30 \text{ \AA}$ and $b = 4.69 \text{ \AA}$. In Fig. 4b we present the atomic structure for disclinated phosphorene crystal Ph5-7v1 after geometry

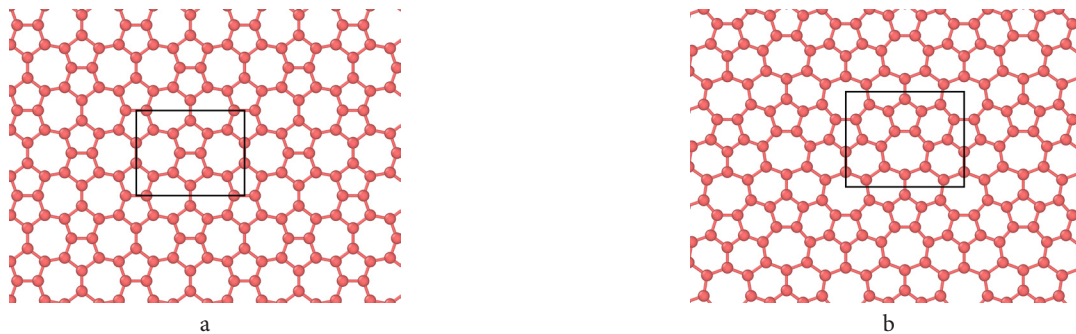


Fig. 3. Lattice structure for pseudo-graphene crystals. G5-7v1 pseudo-graphene crystal (a); and G5-6-7v2 pseudo-graphene crystal (b). Rectangle areas display the lattice unit cells.

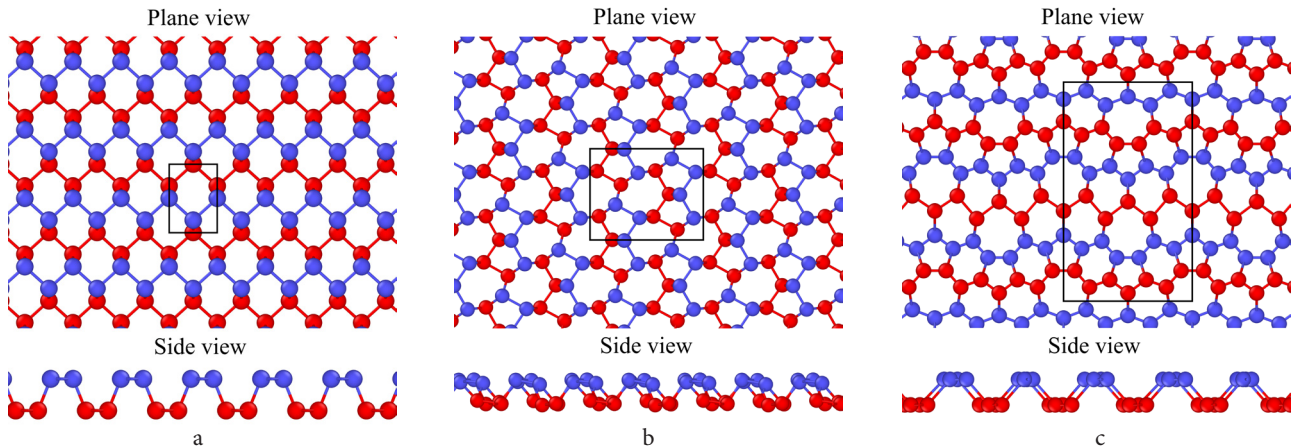


Fig. 4. (Color online) Lattice structure for pristine and disclinated phosphorenes. Pristine phosphorene (a); Ph5-7v1 disclinated phosphorene (b); Ph5-6-7v2 disclinated phosphorene (c). Rectangle area displays the lattice unit cell. Blue and red colors correspond to top and bottom atomic levels, respectively.

optimization; its crystal lattice parameters are $a=9.30 \text{ \AA}$ and $b=7.50 \text{ \AA}$. Figure 4c shows the crystal lattice for the disclinated phosphorene crystal Ph5-6-7v2 after geometry optimization; it possesses lattice parameters $a=12.39 \text{ \AA}$ and $b=21.55 \text{ \AA}$.

The results of DFT calculations confirm that both of modelled 2D disclinated phosphorus-based materials have stable crystal lattices. This means that such 2D structures can be potentially synthesized.

5. Electronic band structure of disclinated phosphorene

Figure 5 presents the band structure diagrams calculated within DFT analysis for the materials under consideration.

It is known that phosphorene is a direct-gap semiconductor with a band gap of 0.91 eV [32]. Our DFT calculations for pristine phosphorene confirmed this result with slightly different value of the band gap 0.86 eV, see Fig. 5a, that indicates an overall correctness of the chosen simulation parameters. Our calculations show that disclinated phosphorenes are characterized by a qualitative change in the band diagram, which transforms to the indirect band gap case for Ph5-7v1 (band gap is 1.24 eV, see Fig. 5b) and to the metal-like behavior for Ph5-6-7v2 (without band gap, see Fig. 5c).

It should be noted that the electronic band structure of previously proposed polymorphic forms of phosphorene was found to be either in the form typical to indirect band gap semiconductors (ζ -P, η -P, θ -P), or direct band gap semiconductor (ε -P), or metal without band gap ($\gamma\varepsilon$ -P) [19]. The ε -P polymorph consists of only 4- and 8-member defective phosphorus rings, retaining an ordered two-level structure, as in phosphorene. In contrast, the polymorphic form ζ -P, although consists of only 4- and 8-member defective phosphorus rings, transforms from a two-level structure to a single-level one, where the crystal is bent in a zigzag in the

third dimension. The $\gamma\varepsilon$ -P polymorph has a similar zigzag lattice in the third dimension, but its lattice, in addition to defective rings, has deformed 6-member phosphorus rings. Polymorphs η -P and θ -P deviate from the usual structure of phosphorene, having in their lattice defective 7- member and 5- member rings. In this last case, they form closed ribbons in the material, where defective rings are stacked into chains and then assembled into a layer with large pores.

When we consider the changes in the band structure of carbon based materials we find that pseudo-graphene crystals G5-7v1 and G5-6-7v2 have a Dirac cone in their band structure diagram, as well as pristine graphene [26]. Thus, for disclinated graphene with a similar disclination network, no qualitative changes are observed, in contrast to the disclinated phosphorene case. This can be explained by the fact that phosphorene has a two-level atomic structure.

6. Summary and conclusions

Exploring simulation data for pseudo-graphene crystals, the lattice design for disclinated phosphorenes has been compiled. The analysis of the designed structures has been performed using the density functional theory. The DFT analysis has confirmed stability of the modelled disclinated phosphorenes. It has been found that Ph5-7v1 disclinated phosphorene demonstrates the indirect band gap, in contrast to the direct-gap pristine phosphorene, whereas Ph5-6-7v2 disclinated phosphorene has a metal-like band structure.

For the future, we plan to conduct detailed studies of disclinated phosphorenes exploring both DFT calculations and molecular dynamic (MD) method for the analysis of thermal and mechanical properties. It will be also possible to transfer already described pseudo-graphene lattices to a wide class of 2D non-carbon materials.

Acknowledgements. The work was supported by the Russian Science Foundation (grant No 19-19-00617).

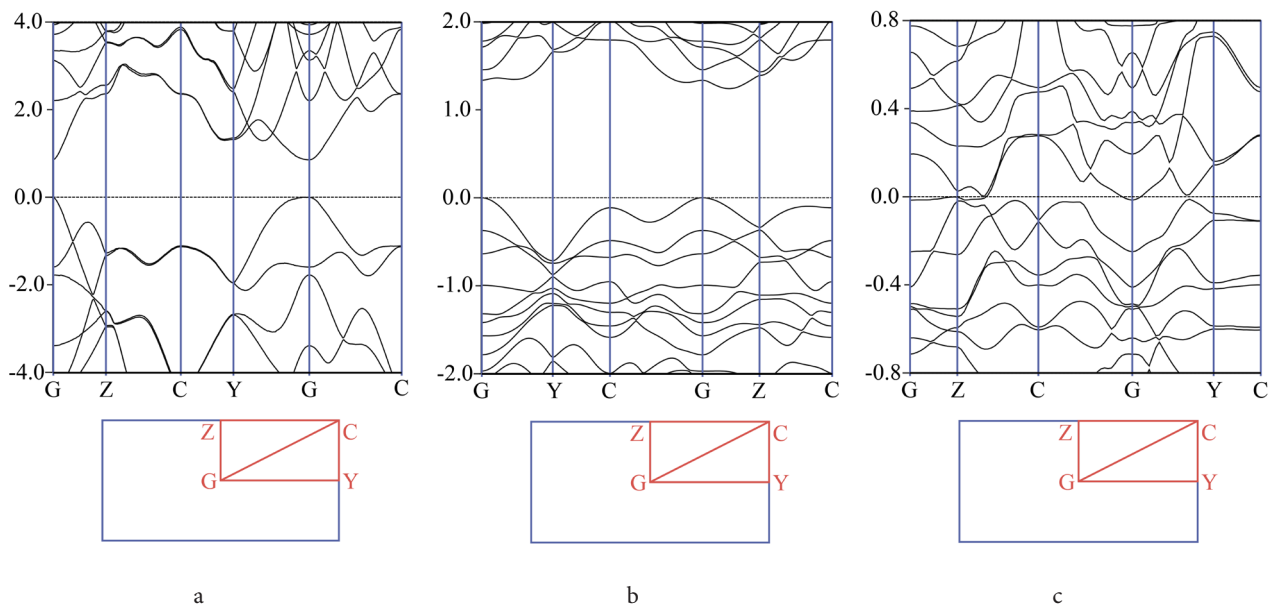


Fig. 5. (Color online) Electronic band structure for modelled pristine and disclinated phosphorenes. Pristine phosphorene (a); Ph5-7v1 disclinated phosphorene (b); Ph5-6-7v2 disclinated phosphorene (c). Rectangle area displays first Brillouin zone.

References

1. G.R. Bhimanapati, Z. Lin, V. Meunier, Y. Jung, J. Cha, S. Das, D. Xiao, Y. Son, M. S. Strano, V.R. Cooper, L. Liang, S.G. Louie, E. Ringe, W. Zhou, S.S. Kim, R.R. Naik, B.G. Sumpter, H. Terrones, F. Xia, Y. Wang, J. Zhu, D. Akinwande, N. Alem, J.A. Schuller, R.E. Schaak, M. Terrones, J.A. Robinson. *ACS Nano*. 9 (12), 11509 (2015). [Crossref](#)
2. S. Balendhran, S. Walia, H. Nili, S. Sriram, M. Bhaskaran. *Small*. 11 (6), 640 (2015). [Crossref](#)
3. H. Liu, Y. Du, Y. Deng, P.D. Ye. *Chem. Soc. Rev.* 44 (9), 2732 (2015). [Crossref](#)
4. M. Chhowalla, D. Jena, H. Zhang. *Nat. Rev. Mater.* 1 (11), 16052 (2016). [Crossref](#)
5. A. Carvalho, M. Wang, X. Zhu, A.S. Rodin, H. Su, A.H. Castro Neto. *Nat. Rev. Mater.* 1 (11), 16061 (2016). [Crossref](#)
6. K.S. Novoselov, A.K. Geim, S.V. Morozov, D. Jiang, M.I. Katsnelson, I.V. Grigorieva, S.V. Dubonos, A.A. Firsov. *Nature*. 438 (7065), 197 (2005). [Crossref](#)
7. S. Chen, A.L. Moore, W. Cai, J.W. Suk, J. An, C. Mishra, C. Amos, C.W. Magnuson, J. Kang, L. Shi, R.S. Ruoff. *ACS Nano*. 5 (1), 321 (2011). [Crossref](#)
8. C. Lee, X. Wei, J.W. Kysar, J. Hone. *Science*. 321 (5887), 385 (2008). [Crossref](#)
9. A.E. Romanov, A.L. Kolesnikova, T.S. Orlova, I. Hussainova, V.E. Bougrov, R.Z. Valiev. *Carbon*. 81, 223 (2015). [Crossref](#)
10. A.E. Romanov, M.A. Rozhkov, A.L. Kolesnikova. *Lett. Mater.* 8 (4), 384 (2018). [Crossref](#)
11. N.D. Abramenko, M.A. Rozhkov, A.L. Kolesnikova, A.E. Romanov. *Rev. Adv. Mater. Technol.* 2 (4), 9 (2020). [Crossref](#)
12. L. Tapasztó, P. Nemes-Incze, G. Dobrik, K. Jae Yoo, C. Hwang, L.P. Biró. *Appl. Phys. Lett.* 100 (5), 053114 (2012). [Crossref](#)
13. Q. Fan, L. Yan, M.W. Tripp, O. Krejčí, S. Dimosthenous, S.R. Kachel, M. Chen, A.S. Foster, U. Koert, P. Liljeroth, J.M. Gottfried. *Science*. 372 (6544), 852 (2021). [Crossref](#)
14. Y. Luo, C. Ren, Y. Xu, J. Yu, S. Wang, M. Sun. *Sci. Rep.* 11 (1), 19008 (2021). [Crossref](#)
15. N. Narita, S. Nagai, S. Suzuki, K. Nakao. *Phys. Rev. B*. 58 (16), 11009 (1998). [Crossref](#)
16. Z. Wang, X.-F. Zhou, X. Zhang, Q. Zhu, H. Dong, M. Zhao, A.R. Oganov. *Nano Lett.* 15 (9), 6182 (2015). [Crossref](#)
17. W. Hu, J. Yang, *J. Phys. Chem. C*. 119 (35), 20474 (2015). [Crossref](#)
18. M. Wang, R. Song, X. Zhang, G. Liu, S. Xu, Z. Xu, J. Liu, G. Qiao. *Int. J. Hydrogen Energy*. 46 (2), 1913 (2021). [Crossref](#)
19. M. Wu, H. Fu, L. Zhou, K. Yao, X. C. Zeng. *Nano Lett.* 15 (5), 3557 (2015). [Crossref](#)
20. J. Ma, D. Alfè, A. Michaelides, E. Wang. *Phys. Rev. B — Condens. Matter Mater. Phys.* 80 (3), 033407 (2009). [Crossref](#)
21. A.E. Romanov, V.I. Vladimirov. *Phys. Status Solidi*. 78 (1), 11 (1983). [Crossref](#)
22. A.E. Romanov, A.L. Kolesnikova. *Prog. Mater. Sci.* 54 (6), 740 (2009). [Crossref](#)
23. M.A. Rozhkov, A.L. Kolesnikova, I.S. Yasnikov, A.E. Romanov. *Low Temp. Phys.* 44 (9), 918 (2018). [Crossref](#)
24. M.A. Rozhkov, A.L. Kolesnikova, T.S. Orlova, L.V. Zhigilei, A.E. Romanov. *Mater. Phys. Mech.* 29 (1), 101 (2016).
25. J.P. Hirth, J. Lothe. *Theory of Dislocations*. Second Ed. Krieger publishing company, Malabar, Florida (1982).
26. M.A. Rozhkov, A.L. Kolesnikova, I. Hussainova, M.A. Kaliteevskii, T.S. Orlova, Y.Y. Smirnov, I.S. Yasnikov, L.V. Zhigilei, V.E. Bougrov, A.E. Romanov. *Rev. Adv. Mater. Sci.* 57 (2), 137 (2018). [Crossref](#)
27. A.N. Enyashin, A.L. Ivanovskii. *Phys. Status Solidi*. 248 (8), 1879 (2011). [Crossref](#)
28. Quantum Espresso. Available [online](#): (accessed on 1 Nov. 2022).
29. N.D. Abramenko, M.A. Rozhkov. *Rev. Adv. Mater. Technol.* 3 (4), 19 (2021). [Crossref](#)
30. Y. Baskin, L. Meyer. *Phys. Rev.* 100 (2), 544 (1955). [Crossref](#)
31. L. Lindsay, D.A. Broido. *Phys. Rev. B*. 81 (20), 205441 (2010). [Crossref](#)
32. X. Peng, Q. Wei, A. Copple. *Phys. Rev. B*. 90 (8), 085402 (2014). [Crossref](#)